

The influence of municipal solid waste incinerator fly ash slag blended in cement pastes

Kae-Long Lin*

Department of Environmental Engineering, National I-Lan University, I-Lan 260, Taiwan, ROC

Received 30 May 2003; accepted 7 June 2004

Abstract

This study investigates the effect of mixing Type I, Type II, and Belite cements with municipal solid waste incinerator (MSWI) fly ash slag-blended cement (FASBC). The experimental results showed that a 10–40% slag replacement of by caused an increase in the initial and the final setting time. The toxicity characteristic leaching procedure (TCLP) results show that the heavy metal content met the Environmental Protection Administration (EPA) regulatory limits. From the results, it can be seen that the effect of the replacement of 10–40% of the cement by slag caused an increase in the initial and final setting time. Compressive strength results indicate that the slag-blended cement (SBC) pastes had slower compressive strength development in the early stages, but this strength obviously increased at later ages. Variations in the Portland cements can affect early strength development but have no significant effect on the degree of hydration at later ages. MSWI slag gives a relatively slower increase in early strength but may show a greater degree of reaction at later ages.

© 2004 Elsevier Ltd. All rights reserved.

Keywords: Heavy metal; Compressive strength; Hydration; Portland cement

1. Introduction

According to Taiwan Environmental Protection Administration (Taiwan EPA) statistics, by the year 2004, there will be more than 3000 metric tons of incinerator residues (including bottom ash, fly ash, and scrubber ash, in here referred to as incinerator ashes) discharged from municipal solid waste incinerators (MSWIs) island-wide daily. Taiwan EPA regulation classifies MSWI bottom ash as nonhazardous, but the fly ash as hazardous. This hazardous fly ash has to be detoxified or disposed of in a secure landfill. Their treatment/disposal and environmental impact has become a major public concern.

The melting of MSWI ash, especially fly ash, has recently been recommended by the Japanese EPA as a feasible disposal alternative for the treatment and recovery of toxic MSWI incinerator fly ash. This process involves melting the MSWI fly ash at temperatures higher than 1300 °C, followed by water-quenching or air-cooling of the molten ash to produce glassy slag. Vittrification technology has been identified as a potentially effective tool for immobilizing heavy metals into nonleachable slag [1,2]. This technology involves subjecting the waste material to high temperatures, so that the

nonvolatile species become chemically bonded in the resultant matrix, known as slag, thereby rendering it nonleachable [3]. The resultant slag is reduced in volume, is stable, and is heavy metal leach-resistant [4]. The slag has been utilized as an ingredient in ceramics, aggregates [5], water-permeable bricks, and pavement bricks [6] in Japan. The slag contains calcium aluminates and calcium silicates, which are converted from the related Si, Al, and Ca compounds in the ash, and these can be recovered and can function as a pozzolanic material.

The present study is based on previous research on MSWI fly ash slag-blended cement (FASBC) in which a w/b ratio of 0.38 was used [7,8]. Thus, the present work, the effects of the MSWI fly ash slag, the limited extent, the variations in the amount of the Portland cement (Type I, Type II, or Belite cement), and the slag-blended cement (SBC) pastes are examined.

2. Materials and methods

2.1. Preparation of MSWI fly ash slag

Table 1 indicates the chemical and other types of analyses for the Portland cements and the slag used.

* Tel.: +886-3-935-7400; fax: +886-3-936-7642.

E-mail address: klilin@niu.edu.tw.

Table 1
Chemical composition (%) of the fly ash, slag, and cements

	Fly ash	Pulverized slag	Type I cement	Type II cement	Belite cement
<i>Oxides</i>					
CaO	14.7	27.2	64.5	62.6	62.6
SiO ₂	35.8	38.9	21.6	23.3	27.9
Al ₂ O ₃	9.8	23.3	5.3	2.8	2.8
Fe ₂ O ₃	4.91	5.3	3.4	3.2	3.2
Na ₂ O	5.9	1.2			0.23
K ₂ O	5.3	—			0.5
MgO	0.83	3.6	2.25	1.95	3.21
Cl [−]	5.03	0.01			
<i>Constituents</i>					
C ₃ S	—	—	51	44	21
C ₂ S	—	—	23	34	67
C ₃ A	—	—	8	3	2
C ₄ AF	—	—	10	13	10

The fly ash samples used in this study were collected from the cyclone of an MSWI located in the northern part of Taiwan. The incinerator has a daily processing capacity of 1350 metric tons of municipal solid wastes and is equipped with air pollution control devices consisting of a cyclone, an adsorption reactor, and a fabric baghouse filter. The fly ash taken from the cyclone was homogenized and oven-dried at 105 °C for 24 h. After the samples were dried and cooled, they were again ground and homogenized. Finally, the dried pulverized ash was sieved. The fraction passing through a No. 50 mesh was then analyzed to determine its chemical composition (shown in Table 1). The leachability of the MSWI fly ash was then analyzed by the toxicity characteristic leaching procedure (TCLP) test [9].

2.2. Approach

MSWI fly ash slag was prepared by first melting the MSWI fly ash at 1400 °C for 30 min in an electrically heated furnace to obtain slag samples. The resultant samples were water-quenched and further pulverized with a ballmill. The fraction passing through a No. 200 sieve was stored in a desiccator for subsequent characterization and the engineering property experiments.

The pulverized slag samples prepared were then used as a cement replacement, and were blended with Portland cement (Types I and II) and Belite cement, at replacement ratios ranging from 0% to 40%, resulting in three types of SBC. Pastes using the aforementioned blends were prepared with a water-to-binder ratio of 0.38. Test cubes (25.4 × 25.4 × 25.4 mm, 1 × 1 × 1 in.) were prepared according to ASTM C109, followed by a moulding process (ASTM C31-69). The specimens were then demoulded and cured in a container at 97% humidity and at 25 °C for periods ranging from 1 to 90 days. The compressive strength development of specimens of different ages was then measured according to ASTM C39-72. The leachability of the specimens was then analyzed by TCLP testing. The composition of the pulverized slag and mixed cement pastes were analyzed using a Siemens D5000 sequential X-ray diffraction spectrometer (XRD). The compressive strength test samples were terminated at the required testing age with methanol under a vacuum. They were dried at 60 °C for 24 h before the measurements were made. After oven drying, the samples were analyzed with XRD, mercury intrusion porosimetry (MIP), and degree of hydration testing.

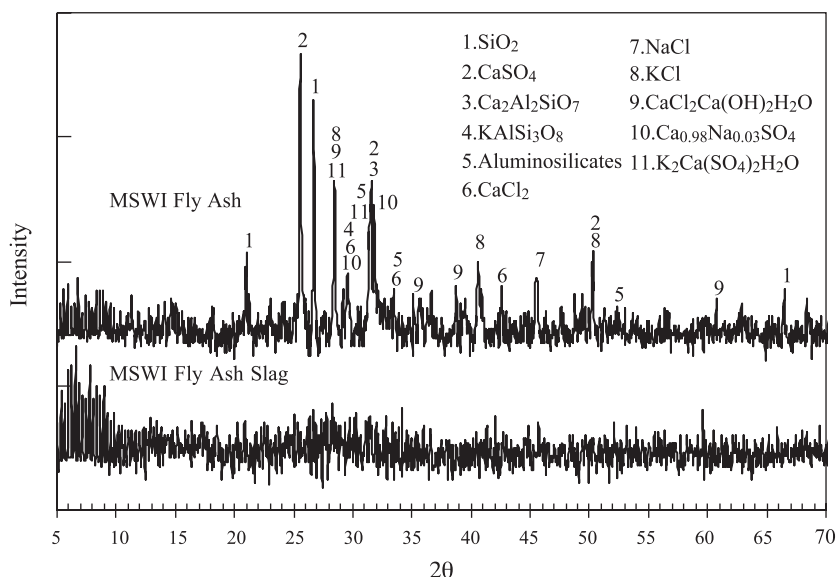


Fig. 1. XRD patterns of MSWI fly ash and slag.

Table 2
TCLP leaching concentration (mg/l) of the MSWI fly ash and slag

Heavy metals	Fly ash	Melting slag	TCLP regulatory limits
Cd	1.8 ± 0.02	ND ^a	1.0
Cr	4.3 ± 0.05	0.27 ± 0.01	5.0
Pb	0.7 ± 0.01	ND ^b	5.0
Cu	0.6 ± 0.01	0.25 ± 0.05	–
Zn	16.2 ± 0.30	14.2 ± 0.33	–

^a Detection limits <0.016 mg/l.

^b Detection limits <0.012 mg/l.

2.3. Sample analysis

Chemical and physical analyses of SBC pastes were conducted at different ages as follows:

- Unconfined compressive strength (UCS): ASTM C109.
- Setting time: The setting times of the cement mixes were determined according to ASTM C191 [10] using a Vicat apparatus at room temperature. The initial setting time occurred when a Vicat needle 1 mm in diameter penetrated the sample to a point 5 ± 1 mm from the bottom of the mould. The final setting time was defined as when a 5-mm cap ring would leave no visible mark when placed on the surface of the sample.
- Heavy metal leachability (TCLP): SW 846-1311.
- Heavy metal concentration: Cd (SW 846-7131A), Pb (SW 846-7421), Zn (SW 846-7951), Cu (SW 864-7211), and Cr (SW 846-7191).
- MIP: A Quantachrome Autoscan MIP was used, with intrusion pressures up to 60,000 psi. By using the Washburn equation, $p = -2\gamma\cos\theta/r$, the pore volume (V) and the corresponding radius (r) were synchronously plotted by an $X-T$ plotter, under the assumption that mercury wetting angle is $\theta = 140^\circ$. In this equation, p , γ , r , and θ stand for the applied pressure, surface tension, pore radius, and wetting angle, respectively.
- Mineralogy: The XRD analysis was carried out by a Siemens D-5000 XRD with $\text{CuK}\alpha$ radiation and 2θ scanning, ranging between 5° and 70° . The XRD scans were run in 0.05° steps, with a 1-s counting time.
- The degree of hydration: The degree of hydration of SBC pastes was determined by thermal analysis [11]. Differential thermal and thermogravimetric analyses

were performed on pastes prepared with a 0.38 water-to-cement weight ratio at various curing ages. The degree of hydration was then calculated as follows:

$$\alpha = \frac{(W_{105} - W_{580}) + 0.41(W_{580} - W_{1007})}{nW_{1007}} \times 100\%,$$

where α is the degree of hydration (%); n is the water completely fixed in the hydrated cement pastes (0.24 for ordinary Portland cement [OPC] paste); W_{105} , W_{580} , and W_{1007} are the sample weights at 150, 580, and 1007 °C, respectively (g); and 0.41 is the conversion factor for the molar ratio of CaCO_3 -derived CO_2 to H_2O .

3. Results and discussion

3.1. Characterization of MSWI fly ash and slag

The properties of the MSWI cyclone ash used in this study were analyzed and are summarized in Table 1. The fly ash was enriched with SiO_2 (35.8%) and CaO (14.7%). It also contains Al_2O_3 (9.8%), Na_2O_3 (5.9%), K_2O (5.3%), and Fe_2O_3 (4.9%). Table 1 lists the major components of the MSWI fly ash slag used in this study. The slag was composed of SiO_2 (39%), CaO (27%), and Al_2O_3 (23%). Fig. 1 shows the speciation of the fly ash, as identified by the XRD techniques. The results indicate that the major components were quartz (SiO_2), anhydrite (CaSO_4), gehlenite ($\text{Ca}_2\text{Al}_2\text{SiO}_7$), anorthite ($\text{CaAl}_2\text{Si}_2\text{O}_8$), microcline (KAlSi_3O_8), calcium chloride (CaCl_2), $\text{CaCl}_2 \cdot \text{Ca}(\text{OH})_2 \cdot \text{H}_2\text{O}$, sylvite (KCl), and halite (NaCl). Fig. 1 shows that the slag contained large amounts of glass, as indicated by the broad diffuse bands between 24° and 37° (2θ).

The TCLP test results are shown in Table 2. High concentrations of zinc, chromium, and cadmium were observed in the fly ash samples. The cadmium concentration was 1.82 mg/l, which exceeded the EPA's regulatory thresh-

Table 3
Setting times (h) of the OPC and SBC pastes incorporating MSWI fly ash slag

Cement	Setting time							
	OPC		10%		20%		40%	
	Initial	Final	Initial	Final	Initial	Final	Initial	Final
Type I	3.68	7.25	3.97	7.75	4.15	8.37	4.86	9.76
Type II	4.35	7.68	4.38	8.20	4.55	8.61	5.27	9.22
Belite	6.20	9.82	6.28	9.93	6.42	10.18	6.88	11.27

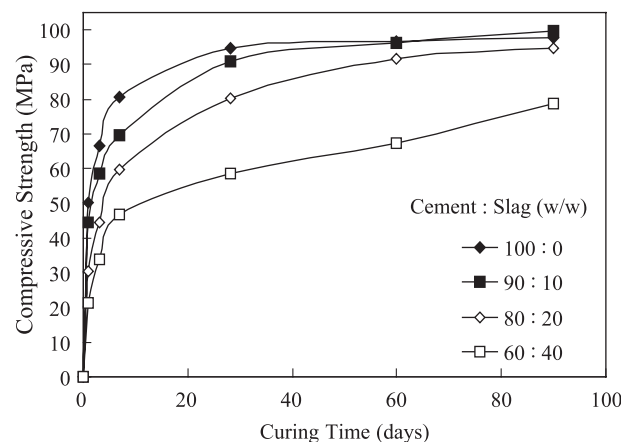


Fig. 2. Compressive strength development of Type I FASBC.

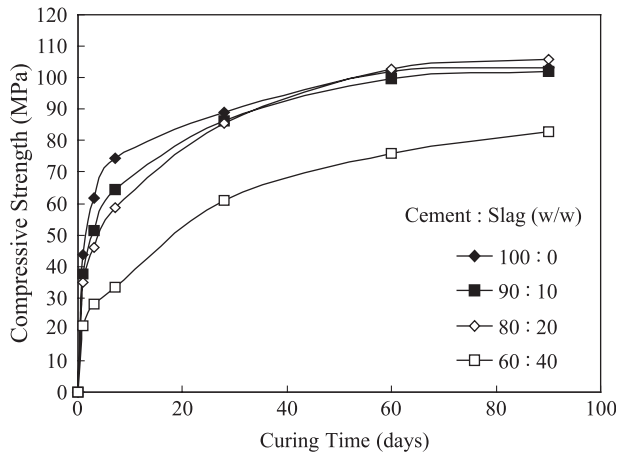


Fig. 3. Compressive strength development of Type II FASBC.

old. The raw MSWI fly ash thus has to be treated before final disposal. On the other hand, the leaching concentrations of the heavy metals in the slag were low, and all met the regulatory threshold. These results indicate the metals were retained in the glassy matrix.

3.2. Setting times

The setting times for the three types of Portland cement pastes, containing different amount of replacement slag are given in Table 3. When the aqueous salts, calcium (Ca) and magnesium (Mg), were introduced to the alkaline silicate solution for alkali-activated cement production, alkali hydroxide precipitates formed almost immediately. On other hand, when the level was high, whether the effects were accelerated or retarded would be dependent on the initial solution composition of the alkali solution. The introduction of aqueous Ca and Mg salt solutions to alkali-activated cement systems can produce many heterogeneous nucleation templates immediately upon their addition. Hence, systems to which Ca and Mg salts have been added should be expected to have

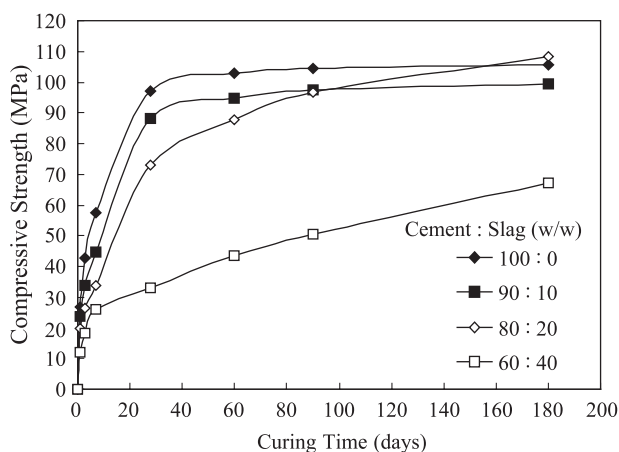


Fig. 4. Compressive strength development of Belite FASBC.

shorter setting times than systems without this addition. Generally, the Mg salts had little effect on the setting while the Ca salts shortened the setting times by varying degrees [12].

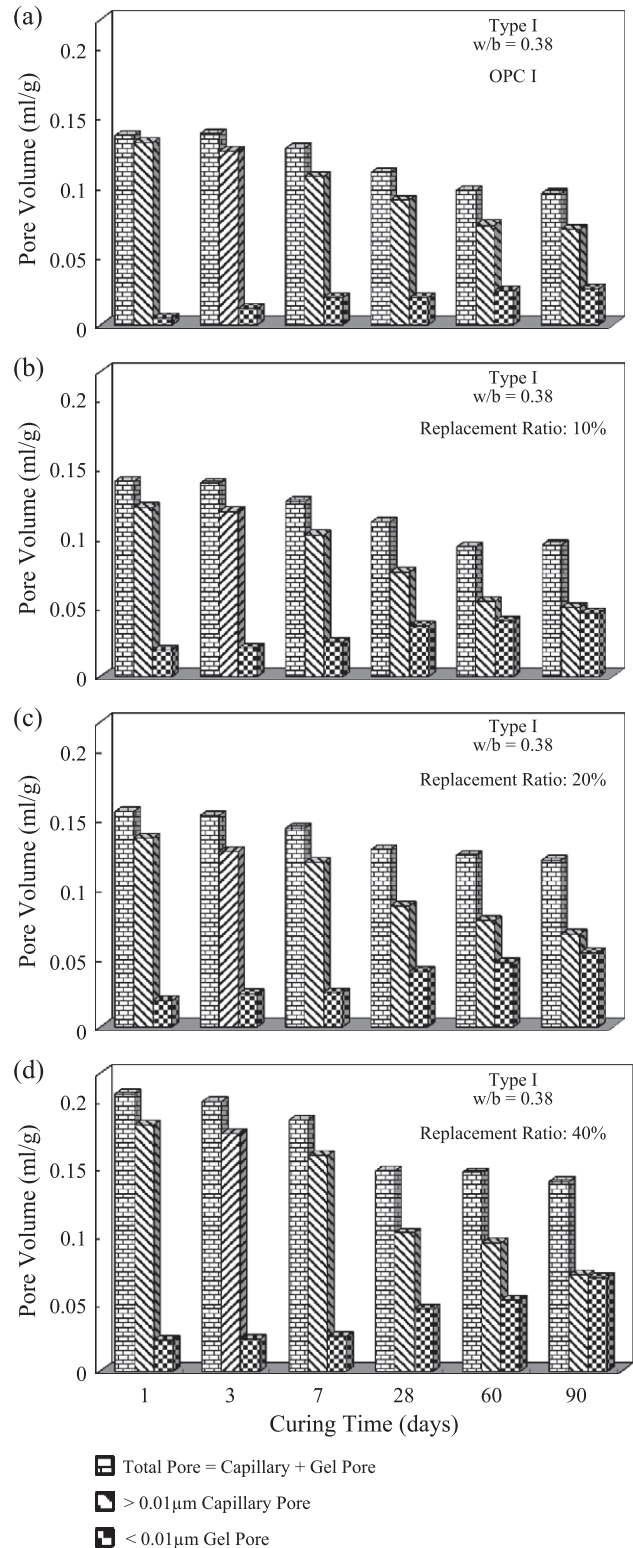


Fig. 5. Porosity distribution of Type I FASBC paste.

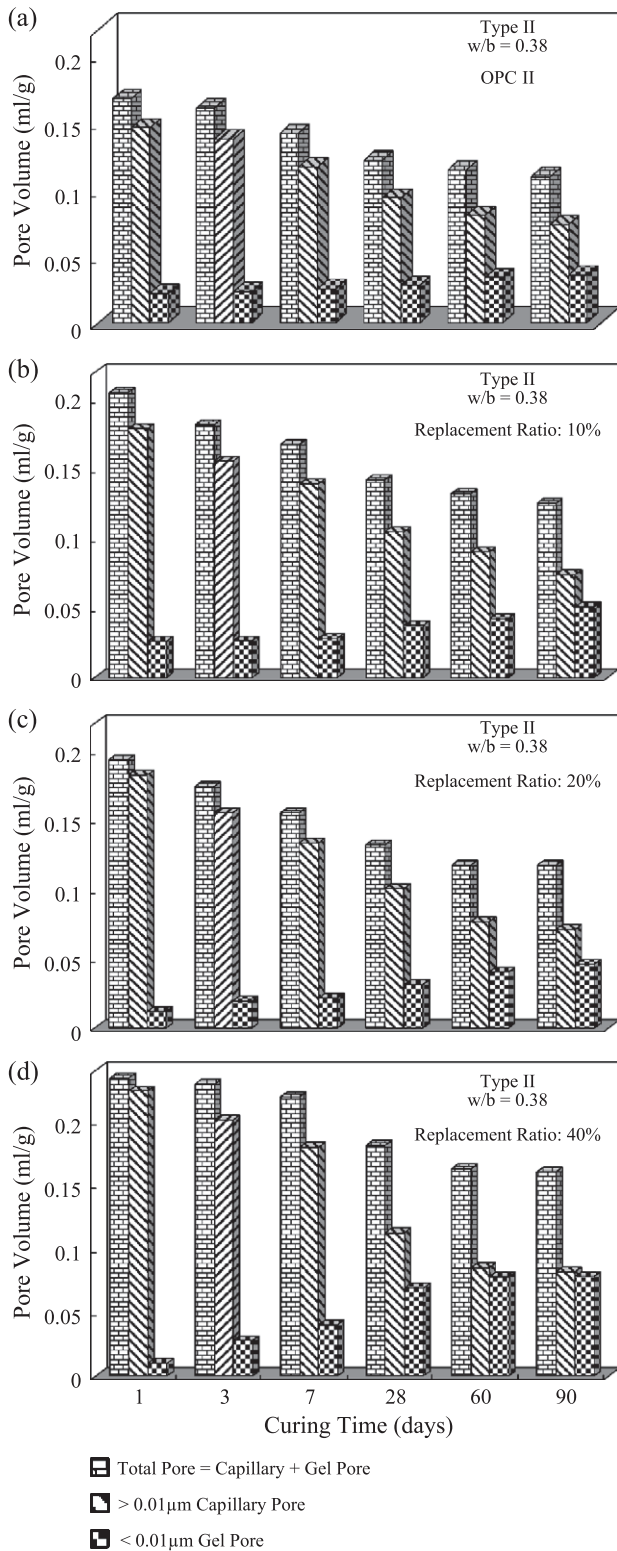


Fig. 6. Porosity distribution of Type II FASBC paste.

From the results, it can be seen that the effect of a 10–40% slag replacement, was an increase in the initial and the final setting times. However, when the replacement level was increased further to 40%, there was a significant increase, particularly in the final setting time, compared with the

control mixture. The observed delay in the setting time may be primarily attributed to the rate of the pozzolanic reactions. Increasing the slag replacement resulted in greater glassiness, and thus delayed the setting time.

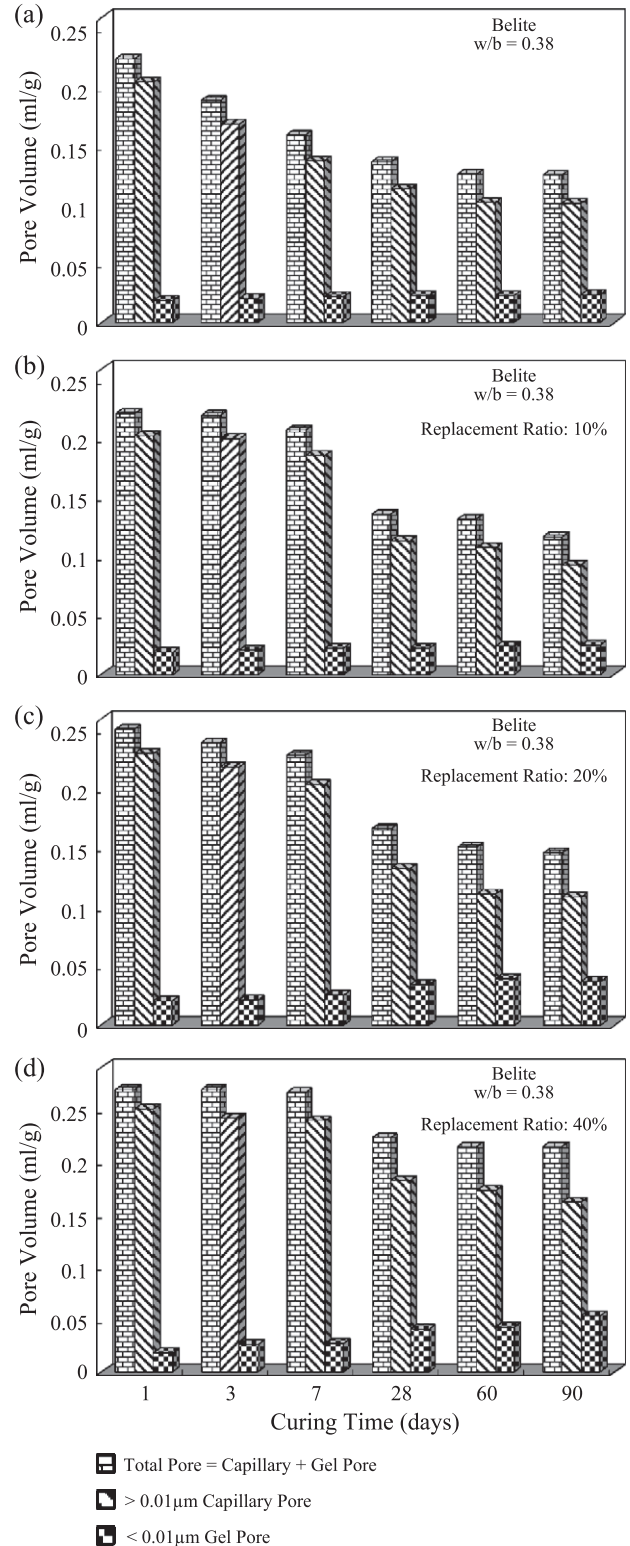


Fig. 7. Porosity distribution of Belite FASBC paste.

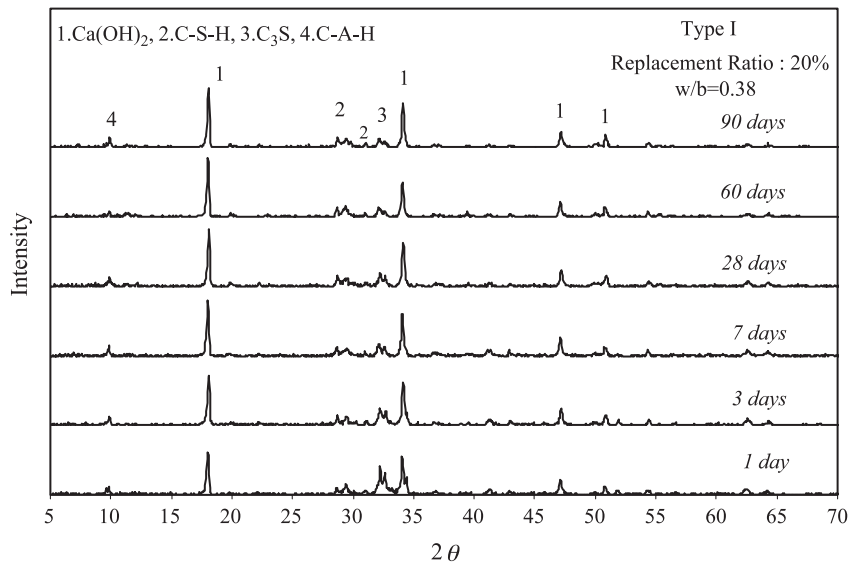


Fig. 8. XRD patterns for Type I SBC paste.

3.3. Compressive strength development in the MSWIFA SBC pastes

Figs. 2–4 show the compressive strength of the MSWIFA SBC Type I, Type II, and Belite cement pastes. It can be observed from these figures that the compressive strengths of all three types of SBC pastes were reduced as the amount of cement replacement increased in the early stages of curing (1–28 days). For longer curing times (60–90 days), with a low amount of cement replacement (10% and 20%), the strength of the SBC pastes reached approximately 110% and 95% to the plain cement paste, respectively. At 90 days, the strength of SBC, with a 10% Type I cement replacement was 2 MPa, which exceeded that of the Type I plain cement paste, whereas the strength of SBC, with a 20% Type II

cement replacement, was 3 MPa. The strength of SBC, with a 20% Belite cement replacement also exceeded 2 MPa. For SBC with 40% of the cement replaced, the strength reached only approximately 75–85%, the strength of the plain cement paste. This could have been due to the dilution effect, which resulted in insufficient calcium hydroxide for pozzolanic reactions. The experimental results indicate that the SBC pastes had a slower compressive strength development in the early stages, but the strength obviously increased at later ages.

3.4. Porosity distribution in MSWIFA SBC pastes

The cumulative porosity for the three types of SBC pastes, obtained from the MIP tests, was used to represent

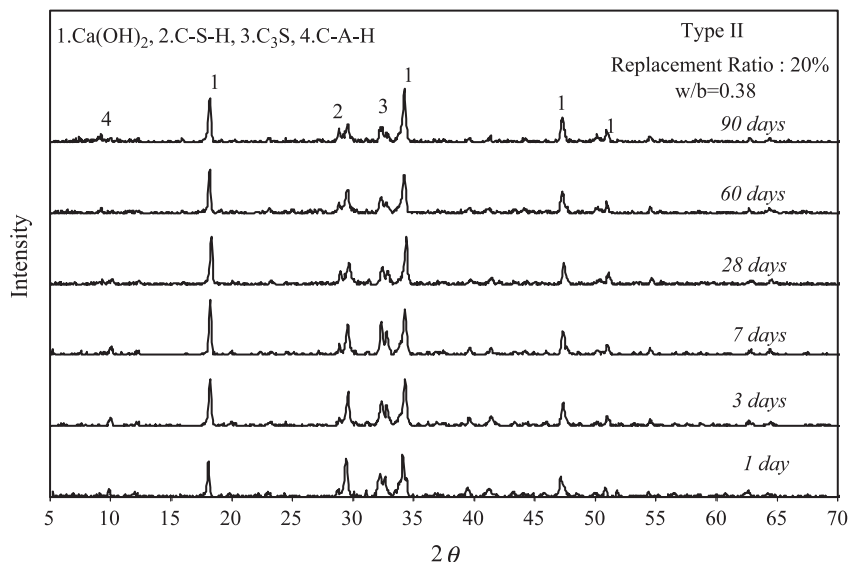


Fig. 9. XRD patterns for Type II SBC paste.

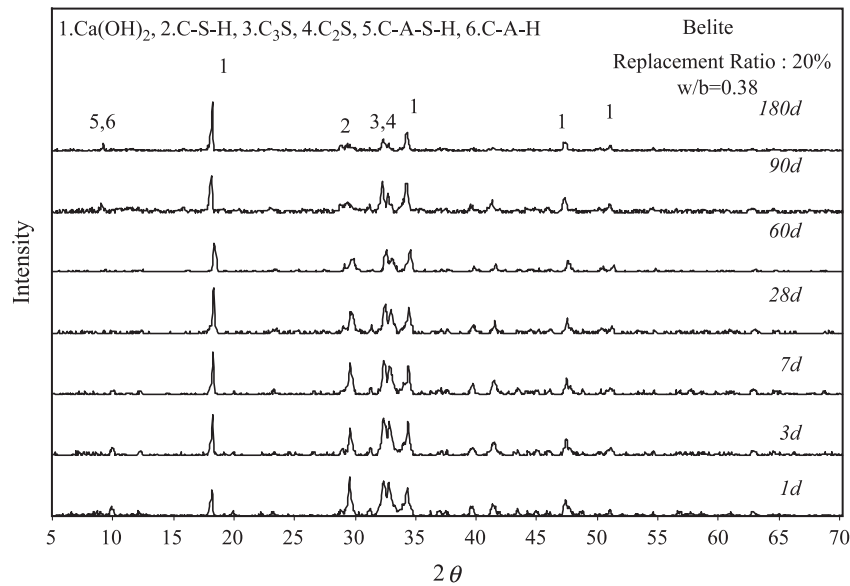


Fig. 10. XRD patterns for Belite SBC paste.

the total paste porosity. The porosities of the Type I, Type II, and Belite SBC pastes are shown in Figs. 5–7, respectively. The capillary pores decreased continuously while the gel pores increased. At a later age (60–90 days), the gel porosity of the SBC pastes increased in volume until higher than that of the plain paste. This could have been due to the presence of the hydration product, calcium silicate hydrates, which occurred during the later pozzolanic reactions, and which filled the capillary pores. The decrease in the capillary pores, in turn, produced greater compressive strength development in the SBC pastes. The increase in the volume of gel pores or micropores with diameters of less than 0.01 μm also indicated that the blended pastes would have better pozzolanic reactions.

3.5. MSWIFA SBC paste hydrates

Figs. 8–10 show the XRD patterns for Type I, Type II, and Belite SBC pastes. Pulverized slag was used to replace 20% of the Type I, Type II, and Belite cement. Fig. 8 XRD analysis has revealed that the C_3S , $\text{Ca}(\text{OH})_2$, calcium aluminum hydrates (CAH) formed in the cement pastes containing MSWI fly ash slag. Fig. 9 shows that in SBC paste with 20% of the Type II cement replaced, $\text{Ca}(\text{OH})_2$, CAH, and residual C_3S were present. Fig. 10 shows that in SBC paste with 20% of the Belite cement replaced, $\text{Ca}(\text{OH})_2$, CAH residual C_3S , and C_2S were present. Kessler et al. have identified the formation of pozzolanic reaction products, in particular stratlingite (C_2ASH_8), in cement pastes containing MSWI fly ash [13]. This hydrate was not identified in our experiments. However, the CAHs were formed. This suggests that the incorporation of fly ash slag had effect on hydration, by the consumption of $\text{Ca}(\text{OH})_2$, due to the formation of the aluminosilicates in the MSWI fly ash slag.

3.6. MSWIFA SBC paste

Table 4 lists the degree of Hydration of the OPC and SBC pastes incorporating MSWI fly ash slag. The paste with 10% of the Type I cement replaced by pulverized slag had a degree of hydration in the paste samples after 90 days of curing time that was less than the plain cement's 2.1% because of the pozzolanic reactions between the activated silicate and aluminum ions in the slag. On the other hand, the SBC with 20% of the Type I cement replaced by pulverized slag, which contained more silicate and aluminum ions, had less $\text{Ca}(\text{OH})_2$ produced after the slag reacted with C_3S and C_2S during the hydration process. The pozzolanic reactions were not complete after 90 days of curing time, which resulted in a 4.6% less degree of hydration than for plain cement. For SBC with 40% of the Type I cement replaced by pulverized slag, the dilution greatly reduced the C_3S , C_3A , and C_2S content in the

Table 4

The degree of hydration (%) of OPC and SBC pastes incorporating MSWI fly ash slag

Paste	Replacement level (%)	Degree of hydration					
		1 day	3 days	7 days	28 days	60 days	90 days
Type I	0	43.6	51.8	59.8	70.0	75.4	83.2
	10	42.5	42.8	59.1	67.7	70.8	81.1
	20	38.0	39.1	53.4	62.0	66.0	78.6
	40	29.0	30.4	43.8	51.9	53.6	61.0
Type II	0	41.7	45.6	49.9	55.5	66.1	69.3
	10	38.5	44.5	46.7	52.0	64.0	67.7
	20	40.1	44.5	44.0	53.8	60.2	64.1
	40	27.0	31.2	35.0	44.6	51.8	58.9
Belite	0	31.0	34.9	40.7	54.3	65.9	68.0
	10	28.4	28.1	35.7	47.8	59.9	61.9
	20	22.8	27.8	31.7	42.4	51.5	53.9
	40	20.9	22.7	29.9	39.8	37.8	38.2

cement, which delayed the hydration process during the early curing stages, as well as the degree of hydration.

The paste with 10% of the Type II cement replaced by pulverized slag did not experience obvious pozzolanic reactions between the activated silicate and aluminum ions in the slag and the C_3S and C_2S in the Type II cement. The degree of hydration of the 90-day sample, although close, was less than plain cement by 2.3%. The SBC with 20% of the cement replaced, since it contained more silicate and aluminum ions, experienced more obvious the pozzolanic reactions with C_2S during the late accelerating hydration process.

The paste with 10% of the Belite cement replaced, since it contained less activated silicate and aluminum ions, showed pozzolanic reactions that due to C_3S hydration-reduction and hydration-enhancement C_2S were not obvious. The degree of hydration of the samples was 6.1% less than that of plain cement. In paste with 40% of the cement replaced, since the hydration of Belite cement is also slow, the addition of a large amount of the pulverized slag greatly reduced the quantity of C_3S , C_3A , and C_2S in the Belite cement, which probably caused the slower development of the degree of hydration.

4. Conclusions

Experiments were conducted using pulverized slag obtained from MSWI fly ash as a pozzolanic material for the replacement of different cements. Based on the above results and discussion, the following conclusions can be drawn:

1. The TCLP results show that the heavy metal content met the EPA regulatory limits.
2. From the results, it can be seen that the affect of the replacement of 10–40% of the cement by slag caused an increase in the initial and final setting time.
3. Variations in the Portland cements could affect early strength development but had no significant effect on the degree of hydration at later ages. MSWI slag that

gives a relatively slower increase in early strength may show a greater degree of reaction at later ages.

4. The degree of hydration of the SBC paste behaved like that of plain paste, increasing with the curing time. The degree of hydration of the slag decreased markedly with decreasing proportion of slags in the blend.

References

- [1] J.W. Sears, R.C. Eschenbach, R.A. Hill, The plasma centrifugal furnace: a method for stabilization and decomposition of toxic and radioactive wastes, *Waste Manage.*, (1990) 165–175.
- [2] I. Joichi, B. Jurgen, Detoxification of municipal waste incineration residues by vitrification, residue treatment, *ABB Rev.* 6/7 (1995) 9–16.
- [3] R. Cortez, H.H. Zaghoul, L.D. Stephenson, E.D. Smith, Laboratory scale thermal plasma arc vitrification studies of heavy metal-laden waste, *J. Air Waste Manage. Assoc.* 46 (1996) 1075–1080.
- [4] M. Nishigaki, Reflecting surface-melt furnace and utilization of the slag, *Waste Manage.* 16 (1996) 445–452.
- [5] S. Abe, F. Kambayashi, M. Okada, Ash melting treatment by rotating type surface melting furnace, *Waste Manage.* 16 (1996) 431–443.
- [6] T. Ito, Vitrification of fly ash by swirling-flow furnace, *Waste Manage.* 16 (1996) 453–460.
- [7] K.S. Wang, K.L. Lin, Z.Q. Huang, Hydraulic activity of municipal solid waste incinerator fly ash slag blended eco-cement, *Cem. Concr. Res.* 31 (2001) 97–103.
- [8] K.L. Lin, K.S. Wang, B.Y. Tzeng, C.Y. Lin, The reuse of municipal solid waste incinerator fly ash slag as a cement substitute, *Resour. Conserv. Recycl.* 39 (4) (2003) 315–324.
- [9] Anonymous, Test Methods for Evaluating Solid Waste, U. S. EPA SW-846, 3rd edition, National Technical Information Service (NTIS), U.S. Department of Commerce, Springfield, MA, 1986.
- [10] S. Targan, A. Olgun, Y. Erdogan, V. Sevinc, Effects of supplementary cementing materials on the properties of cement and concrete, *Cem. Concr. Res.* 32 (2002) 1551–1558.
- [11] B.E. Jazairi, J.M. Illston, The hydration of cement paste using the semi-isothermal method of derivative thermogravimetry, *Cem. Concr. Res.* 10 (1980) 361–366.
- [12] W.K.W. Lee, J.S.J. van Deventer, The effect of ionic contaminants on the early-age properties of alkali-activated fly ash-based cements, *Cem. Concr. Res.* 32 (2002) 577–584.
- [13] S. Remond, D.P. Bentz, P. Pimienta, Effects of the incorporation of municipal solid waste incineration fly ash in cement pastes and mortars: II. Modeling, *Cem. Concr. Res.* 32 (2002) 565–576.